≪Research Paper≫ Applied Science and Convergence Technology Vol.24 No.5, September 2015, pp.156~161
http://dx.doi.org/10.5757/ASCT.2015.24.5.156

Diamagnetic Shift of a InGaP-AlInGaP Semiconductor Single Quantum Well under Pulsed-magnetic Fields

B. K. Choi[a], Yongmin Kim[b]*, and J. D. Song[b]

[a]*Department of Applied Physics and Institute of Nanosensor and Biotechnology, Dankook University, Yongin 16890, Korea*
[b]*Korea Institute of Science and Technology, Seoul 02792, Korea*

(Received September 4, 2015, Revised September 17, 2015, Accepted September 22, 2015)

Application of magnetic fields is important to characterize the carrier dynamics in semiconductor quantum structures. We performed photoluminescence (PL) measurements from an InGaP-AlInGaP single quantum well under pulsed magnetic fields to 50 T. The zero field interband PL transition energy matches well with the self-consistent Poisson-Schrödinger equation. We attempted to analyze the dimensionality of the quantum well by using the diamagnetic shift of the magnetoexciton. The real quantum well has finite thickness that causes the quasi-two-dimensional behavior of the exciton diamagnetic shift. The PL intensity diminishes with increasing magnetic field because of the exciton motion in the presence of magnetic field.

Keywords : Photoluminescence, Magnetic field, Quantum well, Diamagnetic shift

I. Introduction

Research on low dimensional semiconductor quantum structures has long been in the spotlight due to improvements in growth techniques, which have led not only to new scientific effects but also electronic and optoelectronic device applications. Especially, III–V compound semiconductor quantum structures are being used for optoelectronic devices in the visible to near infrared region. Understanding of the carrier dynamics in the semiconductor quantum structures is important before fabricating optoelectronic devices. Even though the devices are operated at room temperature, the carrier dynamics are often studied in the extreme conditions such as low temperature and high magnetic fields because low temperature and high magnetic fields have proved to be powerful tools for investigating the carrier dynamics of the ground and excited states in semiconductor quantum heterostructures.

An exciton in semiconductors is an analogy of the hydrogen atom, wherein a conduction electron (e) and a valence hole (h) consist a bound state. Applying magnetic fields to a semiconductor, the photoexcited $e-h$ pairs consist excitons and they obtain the cyclotron and the diamagnetic energy. The cyclotron energy, which is linear in B, often refers as Landau levels whereas the diamagnetic energy, which is quadratic in B ($\propto B^2$), originate from the cyclotron motion and the binding energy of the exciton (or Rydberg energy, Ry), respectively [1,2]. At low (high) magnetic fields, the exciton binding energy is bigger (smaller) than the cyclotron energy. Therefore, the cyclotron energy

* [E-mail] yongmin@dankook.ac.kr

can be treated as perturbation and vice versa for the high field limit [1,2]. The critical magnetic field, B_C, which divides low and high field limits can be estimated by γ parameter, the ratio of the ground state cyclotron energy to the effective Rydberg energy (Ry^*) to be unity [1],

$$\gamma = \frac{\hbar\omega_c}{2}/Ry^* = \frac{16\pi^2\hbar^3\varepsilon^2\varepsilon_0{}^2}{\mu^2 e^3}B, \quad (1)$$

where ε_0, and ε are the static dielectric constant of vacuum and a given semiconductor, respectively, $1/\mu = 1/m_e + 1/m_h$ is the effective reduced mass of an exciton (m_e and m_h are the effective masses of the conduction electron and the valence hole), and $\omega_c = eB/\mu$ is the cyclotron frequency. Therefore, the critical field, B_C, becomes,

$$\gamma = 1 \rightarrow B_c = \frac{\mu^2 e^3}{16\pi^2\hbar^3\varepsilon^2\varepsilon_0{}^2}. \quad (2)$$

In this paper, we report exciton diamagnetic shift of an InGaP-AlInGaP single quantum well (SQW) under pulsed magnetic fields to 50 T. We attempted to calculate band structure and confined energy levels of the given SQW and compared to the experimental results at zero magnetic field. In the presence of magnetic fields, we extracted the diamagnetic energy shift from the photoluminescence (PL) spectra. We will discuss about the diamagnetic energy shift and PL intensity behaviors under high magnetic fields.

II. Experiments

The InGaP-AlInGaP single quantum well used for this study was grown by using the molecular beam epitaxy technique. The inset of Fig. 1 shows a schematic of the sample structure and the growth sequence of the sample is as follows: Initially, an undoped GaAs (1.0 μm) buffer layer was deposited to release the strain on top of the Si-substrate and a lattice matched undoped AlInP (100 nm) buffer layers were sequentially grown on the GaAs buffer layer. The 8 nm $In_{0.49}Ga_{0.51}P$ SQW, which was sandwiched between the 50 nm $(Al_{0.4}Ga_{0.6})_{0.51}In_{0.49}P$ digital barriers was grown on the AlInP buffer layer. An undoped 50-nm AlInP-alloy capping layer was deposited on the uppermost barrier. Each digital type barrier was grown by using the short period superlattice (SPS) technique [4,5] consisted of 32 SPS layers of $In_{0.49}Al_{0.51}P$ (0.62 nm)/$In_{0.49}Ga_{0.51}P$(0.94 nm). Therefore, the achieved average composition of the barriers on each side of the QW is $(Al_{0.4}Ga_{0.6})_{0.51}In_{0.49}P$ with the total thicknesses of 50 nm.

As seen in Fig. 1, the sample was immersed in liquid ^{4}He cryostat and maintained at 4.2 K for the PL

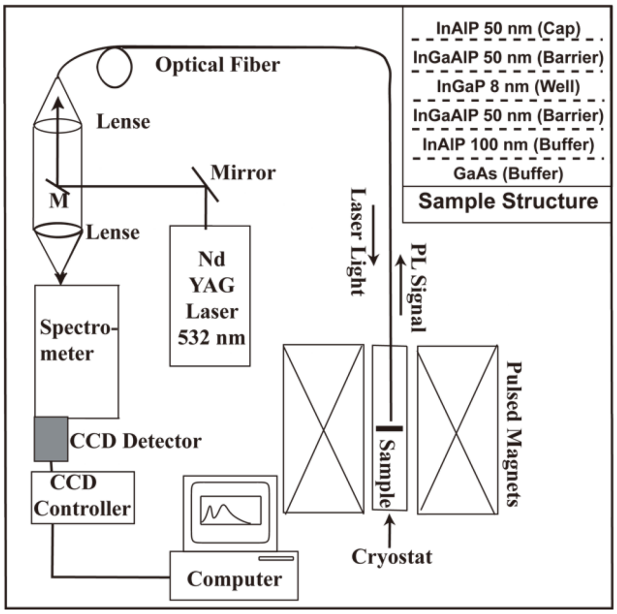

Figure 1. Experimental set up for optical spectroscopic measurements under magnetic fields. A multi-mode optical fiber carries laser light to and photoluminescence signal from the sample located at the center of the magnet. Fast CCD detector system made it possible to take PL spectra during the transient magnetic field pulse. The inset on the right corner depicts the sample structure that was used for this study.

measurements under magnetic fields. The magneto-PL measurements by using a 50 T capacitor-bank-driven pulsed magnet were performed at the International MegaGauss Research Laboratory of the Institute for Solid State Physics (ISSP) at the University of Tokyo. The total transient time of the pulsed magnetic field was ~30 μs. The sample was located at the center of the magnet and a single-mode optical fiber with 1 mm diameter linked the external excitation (laser light) to the sample and the same fiber carries the PL signal back to the spectrometer. The 532-nm line from an Nd-YAG laser was used as the excitation source for the PL measurements, and a 25-cm spectrometer equipped with a liquid-nitrogen-cooled intensified charge-coupled device (ICCD) was used as the detector [6,7].

III. Results and Discussion

To calculate the band structure and the confined energy levels of the sample at low temperature (4 K), we solved the self-consistent nonlinear Poisson-Schrödinger equation under the effective-mass approximation. As seen in Fig. 2, the calculated bandgap between the conduction and the valence band edges (ΔE_G) at the Γ-point is 1.9927 eV. The confined energy levels in the conduction and valence bands from the band-edges are 0.0279 eV and 0.0053 eV. Therefore, the calculated interband energy gap (ΔE_B) becomes 2.0259 eV. The conduction electron and valence bands heavy-hole effective-masses used for the calculation are 0.093 m_0 and 0.819 m_0, respectively, where m_0 is the electron rest mass. As for the wavefunctions, due to the lighter effective-mass, the electron wavefunction in the quantum well smeared out to the barriers more than the valence band heavy-hole wavefunction.

Fig. 3 exhibits the interband transition of the sample from 0 to 50 T under pulsed magnetic fields. At zero magnetic field, the peak position is located at 2.0206 eV which is slightly lower than the calculated value of 2.0259 eV. Such energy difference comes from the exciton binding energy. With increasing magnetic fields, the peak energy position gradually increases and at B=50 T, the peak energy position becomes 2.0281 eV. This blue-shift in magnetic fields is known as the diamagnetic shift. The magnetically obtained energy competes with the electrically confined energy (binding energy). For the weak magnetic field ($B<B_C$), the term that contains the magnetic field in the Schrödinger equation can be treated as a perturbation and the diamagnetic energy shift is quadratic in B ($\Delta E_B \approx e^2 a^2_B B^2/8\mu$) [1,2]. However, when the magnetic field exceeds the critical field

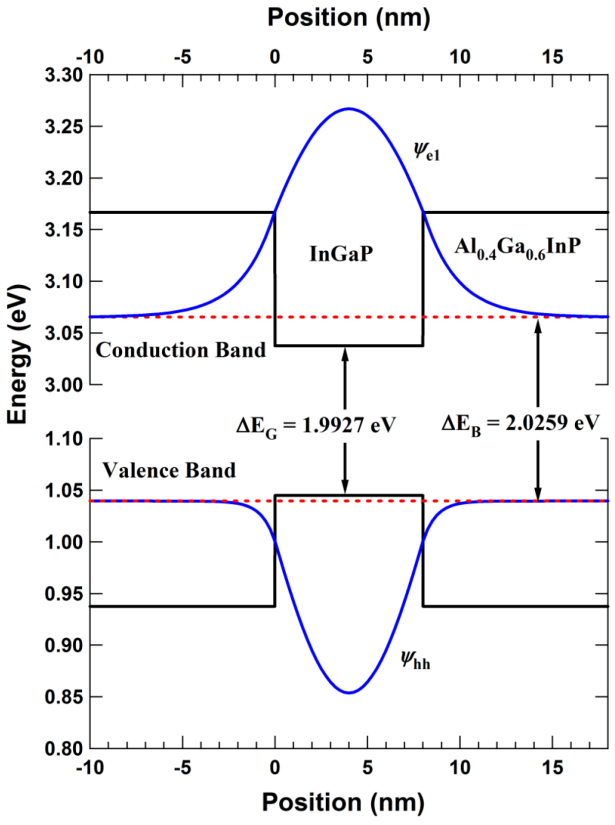

Figure 2. The calculated band structure (solid lines), energy levels (broken lines) and the ground states electron (ψ_{e1}) and heavy-hole wave-functions (ψ_{hh}) of the sample structure by using the self-consistent Poisson Schrödinger equation.

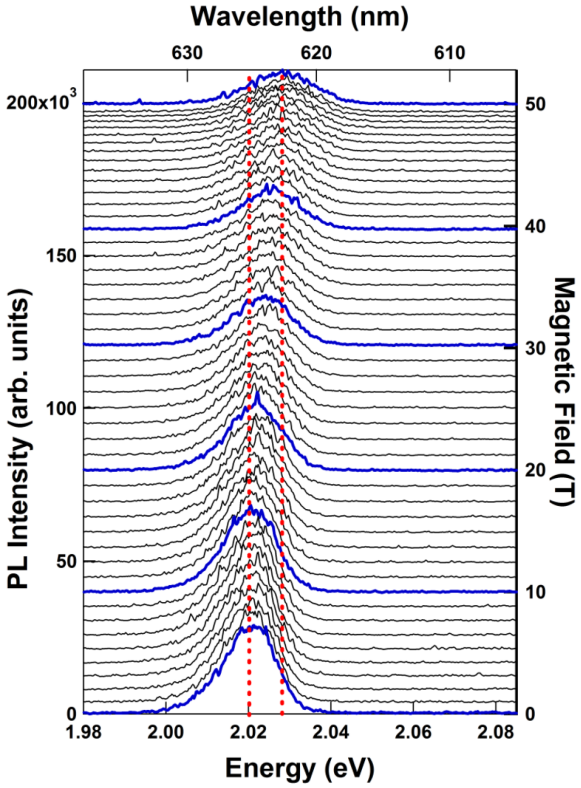

Figure 3. PL spectra in magnetic fields. At B=0, the peak transition energy located at 2.020 eV, which shows blue-shift with increasing magnetic fields (red broken lines).

($B > B_C$), the magnetic energy can no longer be treated as a perturbation and the transition follows the lowest Landau level. The Landau energy is described as $E_n=(n+1/2)\,\hbar\omega_c$ (where n=0, 1, 2, ···). Therefore, the lowest Landau level (n=0) energy becomes $\hbar\omega_c/2=\hbar eB/2\mu$.

Fig. 4 shows the exciton diamagnetic shift (blue open circle) and PL integrated intensity (red solid circle) of the sample in magnetic fields. Before analyzing experimental data, we have to review the basic theoretical model for exciton energy shift in magnetic fields. Empirical equation for the exciton diamagnetic shift can be expressed as [8],

$$\Delta E_B = \frac{\gamma_2 B^2}{1+\alpha B} \quad (entire\ magnetic\ fields). \tag{3-1}$$

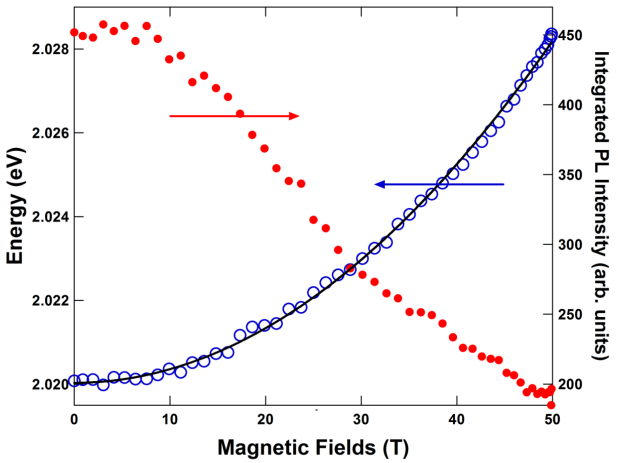

Figure 4. Peak energy (left axis) and integrated PL intensity (right axis) vs. magnetic fields. Solid line is fitting for diamagnetic shift by using Eq. (8).

This equation itself does not contain any physical meaning. However, it provides useful information in the extreme magnetic field limits. At low and high magnetic fields, Eq. (3-1) can be approximated as,

$$\Delta E_B \approx \gamma_2 B^2 = \frac{e^2 a_B^2}{8\mu} B^2 \,(low\ field\ limit, B << B_C), \tag{3-2}$$

and

$$\Delta E_B \approx \frac{\gamma_2}{\alpha} B = \frac{1}{2}\hbar\omega_c = \frac{e\hbar}{2\mu} B \,(high\ field\ limit, B >> B_C), \tag{3-3}$$

$$\alpha = \frac{2\mu\gamma_2}{e\hbar} = \frac{e a_B^2}{4\hbar}, \tag{3-4}$$

where e, μ and a_B is electron charge, effective-reduced-mass of the exciton and effective Bohr radius of the exciton, respectively. By using the InGaP parameters, the exciton effective-reduced-mass (μ) and the Bohr radius (a_B) can be express as,

$$\frac{1}{\mu} = \frac{1}{m_e^*} + \frac{1}{m_{hh}^*} = \frac{1}{0.093 m_0} + \frac{1}{0.819 m_0} = \frac{11.97}{m_0} \text{ and,} \tag{4}$$

$$a_B = \frac{a_0 \varepsilon}{\mu / m_0} = 7.49 \text{ nm}, \tag{5}$$

where a_0=0.0529 nm is the hydrogen Bohr radius. Inserting Eqs. (4) and (5) into Eq. (3-2), the diamagnetic parameter γ_2 becomes,

$$\gamma_2 = \frac{e^2 a_B^2}{8\mu} = 1.476 \times 10^{-5}\ (\mathrm{eV/T^2}). \quad (6\text{-}1)$$

$$\alpha = \frac{2\mu\gamma_2}{e\hbar} = \frac{e a_B^2}{4\hbar} = 2.217 \times 10^{-2}\ /\ \mathrm{T}. \quad (6\text{-}2)$$

Eq. (6-2) is too small to apply the high field limit approximation in Eq. (3-3) within our experimental magnetic fields. Therefore, we applied only Eq. (3-2) for low field limit approximation. Furthermore, Eq. (3-1) valids for three-dimensional (3D) excitons and due to the enhancement of the Rydberg energy in two-dimensional (2D) case, we have to consider a quasi-low-dimensionality of the quantum well before attempting to fit by using Eq. (3-20. This is because the quantum well used for this study has finite well width, which is neither exact-2D nor 3D. Therefore, it is natural that a quasi-2D quantum well with a finite well width has a γ_2 value between the exact 2D and 3D values. For this reason, we introduce dimensional parameter (D) in the following equation, which is unity for 3D and 3/16 for exact-2D quantum wells [2,3].

$$\Delta E_B \approx D\gamma_2 B^2 = D\frac{e^2 a_B^2}{8\mu} B^2. \quad (7)$$

The solid line in Fig. 4 is the fitted curve for diamagnetic shift (blue open circles) by using Eq. (7), and we obtained value for dimensional parameter, D=0.219. The parameter D reflects the size of the Bohr radius of the quasi-2D exicton. Eqs. (3-2) and (7) indicates the relationship between γ_2 and a^2_B for the 3D exciton (a_B(3D)=7.49 nm), the exact-2D exciton a_B(exact－2D)=($\sqrt{3/16}$)a_B=3.24 nm) and qusi-2D case can be estimated as a_B(quasi-2D)=($\sqrt{D}$)a_B= 3.505 nm.

The integrated PL intensity (red solid circle) in Fig. 4 decreases with increasing magnetic fields. This may due to the exciton motion in the presence of magnetic field. The electron (e) and the hole (h) that consist an exciton in a QW undergoes cyclotron motion in opposite circular motion due to the opposite charges under magnetic fields. To cancel the Lorentz force, which is induced by the moving charged particles in magnetic fields, e and h tend to move in opposite linear directions with the same speed. In this respect, the peak positions of the e-h wavefunction tend to shift in opposite direction with increasing magnetic fields. Consequently, overlap between the electron and the hole wavefunctions becomes smaller. This behavior leads to diminish the oscillator strength of the system, which decreases PL intensity with increasing magnetic fields.

IV. Summary

We have undertaken a comprehensive investigation of magnetoexciton in a InGaP single quantum well in pulsed magnetic fields to 50 T at low temperature (4 K). We attempted to calculate the band structure and interband energy gap of the given sample by using the self-consistent Poisson-Schrodinger equation under effective-mass approximation. The calculated interband energy gap is matched well with the experimental value. Under pulsed magnetic fields, which are generated by using the capacitor-bank-driven pulsed magnet at ISSP, the exciton transition energy exhibits the diamagnetic shift. The calculated exact-2D diamagnetic coefficient should be adjusted due to the quasi-2D nature of the magnetoexciton in the QW with a finite width. The integrated PL intensity decreases with increasing magnetic fields. This is due to the consequence of weakening of the oscillator strength by the e-h motion in opposite linear direction to cancel the Lorentz force. We conclude that applying high magnetic fields to

semiconductor heterostructurs provides propound understanding of the exciton dynamics.

Acknowledgements

Work at Dankook University was supported by the National Research Foundation of Korea (NRF 2010-0022383). JDS acknowledges support from the KIST institutional program of flag-ship and partial support by NRF-2013M3C1A3065033. YK thanks to Prof. S. Takeyama and his research group for generous support for using their magnetic field facility.

References

[1] N. Miura, "*Physics of Semiconductors in High magnetic Fields*", (Oxford University Press, New York, 2008) Chap. 2.

[2] D. C. Rogers, J. Singleton, R. J. Nicholas, C. T. Foxon, K. Woodbridge, Phys. Rev. B **34**, 4002 (1986).

[3] Y. Kim, J. Kor. Phys. Soc. **42**, 562 (2003).

[4] Y. H. Shin, Yongmin Kim, J. D. Song, Y. T. Lee, H. Saito, D. Nakamura, Y. H. Matsuda, and S. Takeyama, J. Lum., **151**, 244 (2014).

[5] H. R. Byun, M.-Y. Ryu, J. D. Song, and C. L. Lee, Appl. Sci. Conv. Tech. **23**, 1 (2014).

[6] Y. Kim, Appl. Sci. Conv. Tech. **23**, 1 (2014).

[7] C.H. Perry, Y. Kim, D.G. Rickel, in: Z. Fisk, L. Gorkov, D. Meltzer, R. Schrieffer (Eds.), Physical Phenomena at High Magnetic Fields II, World Scientific, Singapore, 1995, pp. 97-102.

[8] M. Hayne, and B. Bansal, Luminescence **27**, 179 (2012).